

Humpy LNRF-velocity profiles in accretion discs orbiting almost extreme Kerr black holes

A possible relation to quasi-periodic oscillations

Z. Stuchlík, P. Slaný, and G. Török

Institute of Physics, Faculty of Philosophy and Science, Silesian University in Opava, Bezručovo nám. 13, 74601 Opava, Czech Republic
e-mail: zdenek.stuchlik@fpf.slu.cz

Received 18 August 2006 / Accepted 29 November 2006

ABSTRACT

Context. Change of sign of the LNRF-velocity gradient has been found for accretion discs orbiting rapidly rotating Kerr black holes with spin $a > 0.9953$ for Keplerian discs and $a > 0.99979$ for marginally stable thick discs. Such a “humpy” LNRF-velocity profiles occur just above the marginally stable circular geodesic of the black hole spacetimes.

Aims. Aschenbach (2004) has identified the maximal rate of change of the orbital velocity within the “humpy” profile with a locally defined critical frequency of disc oscillations, but it has been done in a coordinate-dependent form that should be corrected.

Methods. We define the critical “humpy” frequency ν_h in general relativistic, coordinate independent form, and relate the frequency defined in the LNRF to the distant observers. At radius of its definition, the resulting “humpy” frequency ν_h is compared to the radial ν_r and vertical ν_v epicyclic frequencies and the orbital frequency of the discs. We focus our attention to Keplerian thin discs and perfect-fluid slender tori where the approximation of oscillations with epicyclic frequencies is acceptable.

Results. In the case of Keplerian discs, we show that the epicyclic resonance radii $r_{3:1}$ and $r_{4:1}$ (with $\nu_v:\nu_r = 3:1, 4:1$) are located in vicinity of the “humpy” radius r_h where efficient triggering of oscillations with frequencies $\sim \nu_h$ could be expected. Asymptotically (for $1 - a < 10^{-4}$) the ratio of the epicyclic and Keplerian frequencies and the humpy frequency is nearly constant, i.e., almost independent of a , being for the radial epicyclic frequency $\nu_r:\nu_h \sim 3:2$. In the case of thick discs, the situation is more complex due to dependence on distribution of the specific angular momentum ℓ determining the disc properties. For $\ell = \text{const.}$ tori and $1 - a < 10^{-6}$ the frequency ratios of the humpy frequency and the orbital and epicyclic frequencies are again nearly constant and independent of both a and ℓ being for the radial epicyclic frequency $\nu_r:\nu_h$ close to 4. In the limiting case of very slender tori ($\ell \sim \ell_{\text{ms}}$) the epicyclic resonance radius $r_{4:1} \sim r_h$ for all the relevant interval of $1 - a < 2 \times 10^{-4}$.

Conclusions. The hypothetical “humpy” oscillations could be related to the QPO resonant phenomena between the epicyclic oscillations in both the thin discs and marginally stable tori giving interesting predictions that have to be compared with QPO observations in nearly extreme Kerr black hole candidate systems. Generally, more than two observable oscillations are predicted.

Key words. black hole physics – accretion, accretion disks – relativity

1. Introduction

High frequency (kHz) twin peak quasi-periodic oscillations (QPOs) with frequency ratios 3:2 (and sometimes 3:1) are observed in microquasars (see, e.g., van der Klis 2000; McClintock & Remillard 2004; Remillard 2005). In the Galactic Center black hole Sgr A*, Genzel et al. (2003) measured a clear periodicity of 1020 s in variability during a flaring event. This period is in the range of Keplerian orbital periods at a few gravitational radii from a black hole with mass $M \sim 3.6 \times 10^6 M_\odot$ estimated for Sgr A* (Ghez 2004). More recently Aschenbach et al. (2004); Aschenbach (2004, 2006) reported three QPO periodicities at 692 s, 1130 s and 2178 s that correspond to frequency ratios $(1/692):(1/1130):(1/2178) \sim 3:2:1$. However, these observational data are not quite convincing, see, e.g. Abramowicz et al. (2004). In some galactic binary black hole and neutron-star systems, the high-frequency QPOs at ν_{high} are accompanied with low-frequency QPOs at ν_{low} . The high-frequency and low-frequency QPOs are correlated and the ratio of the frequencies is observed to be $\nu_{\text{high}}:\nu_{\text{low}} \sim 13:1$. It was first noticed by Psaltis et al. (1999) that the correlation between high-frequencies and

low-frequencies exists for black-hole and neutron-star sources, later Mauche (2002) and Warner et al. (2003) extended this correlation to cataclysmic variables and showed that it is obeyed by high-frequency quasi-coherent “dwarf nova oscillations” and the low-frequency “horizontal branch” oscillations. At present, there is no exact model explaining the ratio 13:1, only a qualitative proposal exists, based on analogy with the 9-th wave from oceanography (Abramowicz et al. 2004). In this concept, the high-frequency QPOs are connected to transient oscillatory phenomena at random locations in the accretion disc and are subject to the side band instability similar to those considered in oceanography (Benjamin & Feir 1967). If a wave pulse contains initially waves of identical length and frequency ν_{high} , nonlinearities can cause the waves with larger amplitude to move faster changing their wavelength. The shorter (longer) waves in front of (behind) the pulse cause energy to concentrate at the center of the pulse feeding thus the instability, the result of which is that every n th wave has a higher amplitude creating low-frequency oscillations with frequency $\nu_{\text{low}} \sim \nu_{\text{high}}/n$. The value of n depends on details of the hydrodynamic models and it

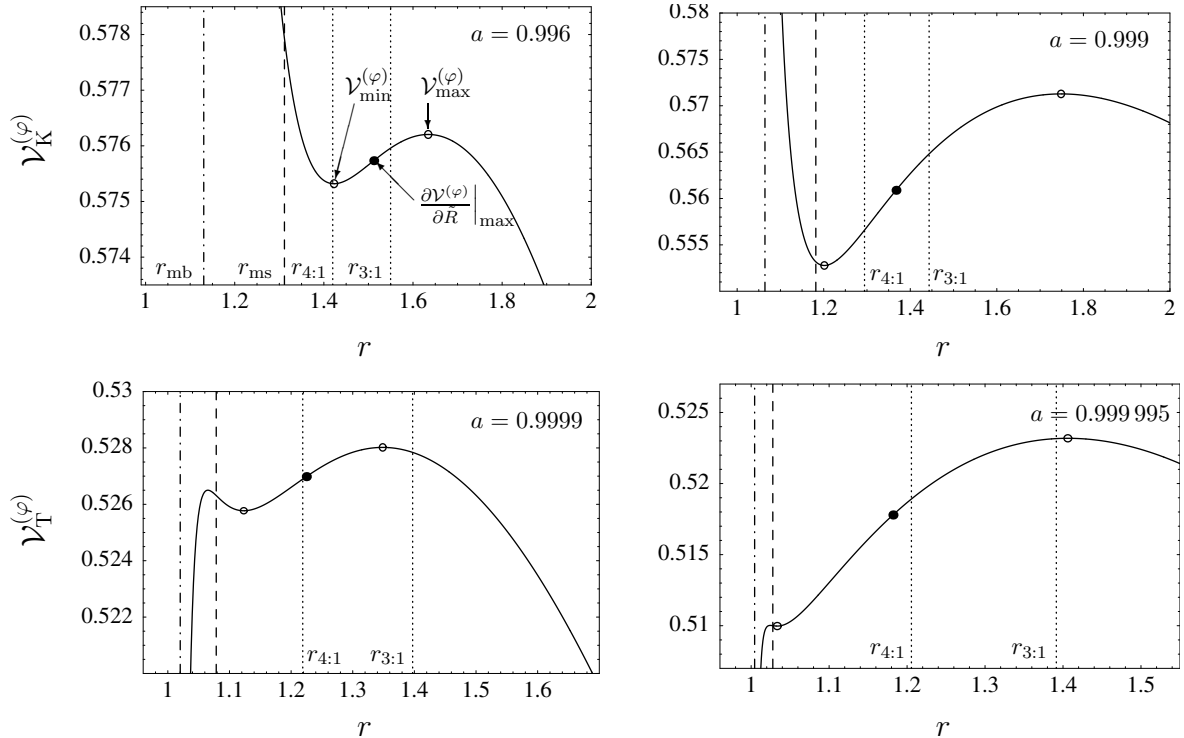


Fig. 1. Profiles of the equatorial orbital velocity related to LNRF in terms of the radial Boyer-Lindquist coordinate for appropriately chosen values of the black-hole spin a in the case of Keplerian discs (*upper plots*) and limiting marginally stable thick discs with $\ell = \ell_{\text{ms}} = \text{const.}$ specific angular momentum distribution (*lower plots*). The resonant orbits $r_{3:1}$ and $r_{4:1}$ of the epicyclic frequencies $\nu_v:\nu_r$ together with the marginally stable (dashed line) and marginally bound (dashed-dotted line) orbits are also given.

is not fully understood in both oceanography (where $n \sim 9$) and discography (where $n \sim 12\text{--}14$; Abramowicz et al. 2004).

It was proposed by Kluźniak & Abramowicz (2001) that the high frequency twin peak QPOs are related to the parametric or forced resonance in accretion discs (Landau & Lifshitz 1973), possibly between the radial and vertical epicyclic oscillations (Aliev & Galtsov 1981; Nowak & Lehr 1998) or the orbital and one of the epicyclic oscillations. These oscillations could be related to both the thin Keplerian discs (Abramowicz et al. 2003; Kato 2001) or the thick, toroidal accretion discs (Rezzolla et al. 2003; Kluźniak et al. 2004a). In particular, the observations of high frequency twin peak QPOs with the 3:2 frequency ratio in microquasars can be explained by the parametric resonance between the radial and vertical epicyclic oscillations, $\nu_v:\nu_r \sim 3:2$. This hypothesis, under the assumption of geodesic oscillations (i.e., for thin discs), puts strong limit on the mass–spin relation for the central black hole in microquasars (Török et al. 2005; Török 2005; Török et al. 2006).

Aschenbach (2004, 2006) discovered that two changes of sign of the radial gradient of the Keplerian orbital velocity as measured in the locally non-rotating frame (LNRF) (Bardeen et al. 1972) occur in the equatorial plane of Kerr black holes with $a > 0.9953$. Stuchlík et al. (2005) have found that the gradient sign change in the LNRF-velocity profiles occurs also for non-geodesic motion with uniform distribution of the specific angular momentum $\ell(r, \theta) = \text{const.}$ (i.e., in marginally stable thick discs) around extremely rapid Kerr black holes with $a > 0.99979$ ¹.

The global character of the phenomenon is given in terms of topology changes of the von Zeipel surfaces (equivalent to equivelocity surfaces in the tori with $\ell(r, \theta) = \text{const.}$). Toroidal von Zeipel surfaces exist around the circle corresponding to the minimum of the equatorial LNRF-velocity profile, indicating possibility of development of some instabilities in that part of the marginally stable disc with positive gradient of the orbital velocity in LNRF (Stuchlík et al. 2004, 2005).

Therefore, we consider the positive radial gradient of orbital LNRF-velocity around black holes with $a > 0.9953$, see Fig. 1, to be a physically interesting phenomenon, even if a direct mechanism relating this phenomenon to triggering the oscillations, and subsequent linking of the oscillations to the excitation of radial (and vertical) epicyclic oscillations, is unknown. We present a basic study of the “humpy” oscillatory frequency and its relation to the epicyclic and Keplerian (orbital) frequencies. It should be stressed that recently at least two QPOs sources are observed, in which the rotational parameter (spin) of the central black hole is estimated nearly extreme, i.e., $a > 0.99$. Such black holes are probably observed in Sgr A* (Aschenbach 2006) and in GRS 1915+105 (McClintock et al. 2006). We plan to make a detailed analysis of the observed frequencies and their possible relation to the LNRF-velocity hump induced frequency and related epicyclic frequencies in the future work.

Aschenbach (2004, 2006), considering phenomena observed in Sgr A*, has shown that in the field of the Kerr black hole with $a \simeq 0.99616$, the orbit where the critical frequency subjected to the hump of the LNRF-velocity profile in such a way that the positive rate of change of the LNRF-velocity is maximal, $(v_{\text{crit}}^A = \partial v^{(\varphi)} / \partial r)_{\text{max}}$, is located nearby $r = r_{3:1}$, where the vertical and radial epicyclic frequencies are in the ratio of $\nu_v:\nu_r = 3:1$ and, moreover, the critical frequency v_{crit}^A is nearly equal to the radial epicyclic frequency there. Undoubtedly, this is

¹ Note that the assumption of uniform distribution of the specific angular momentum can be relevant at least at the inner parts of the thick disc and that matter in the disc follows nearly geodesic circular orbits nearby the center of the disc and in the vicinity of its inner edge determined by the cusp of its critical equipotential surface (see, Abramowicz et al. 1978).

an interesting result. However, the critical frequency introduced by Aschenbach is related to the rate of change of the locally measured orbital velocity in terms of the special Boyer-Lindquist radial coordinate, so the coincidence $v_{\text{crit}}^A \simeq v_r$ obtained in this case is rather unrealistic. In this paper we give the critical frequency v_{crit}^R , related to the maximal positive radial gradient of the LNRF-velocity in the “humpy” velocity profile, in the general relativistic, coordinate-independent form. Further, since the critical frequency v_{crit}^R is defined locally, being connected to the LNRF, it has to be transformed into the form related to distant stationary observers, giving observationally relevant frequency $v_h = v_{\infty}^R$.

In Sect. 2, we briefly summarize properties of the Aschenbach effect for Keplerian thin discs, and $\ell = \text{const.}$ thick discs. In Sect. 3, the critical frequency, connected to the LNRF-velocity positive gradient in the humpy profiles, is given in the physically relevant, coordinate independent form for the both Keplerian and $\ell = \text{const.}$ discs. At the radius of its definition, the critical frequency is compared to the radial and vertical epicyclic frequency and the orbital frequency. In Sect. 4, the results are discussed and concluding remarks are presented.

2. LNRF-velocity profiles of discs orbiting the Kerr black holes

In the Kerr spacetimes with the rotational parameter assumed to be $a > 0$, the relevant metric coefficients in the standard Boyer-Lindquist coordinates read:

$$g_{tt} = -\frac{\Delta - a^2 \sin^2 \theta}{\Sigma}, \quad g_{t\varphi} = -\frac{2ar \sin^2 \theta}{\Sigma}, \quad (1)$$

$$g_{\varphi\varphi} = \frac{A \sin^2 \theta}{\Sigma}, \quad g_{rr} = \frac{\Sigma}{\Delta}, \quad g_{\theta\theta} = \Sigma, \quad (2)$$

where

$$\Delta = r^2 - 2r + a^2, \quad \Sigma = r^2 + a^2 \cos^2 \theta, \quad (3)$$

$$A = (r^2 + a^2)^2 - \Delta a^2 \sin^2 \theta. \quad (4)$$

The geometrical units, $c = G = 1$, together with putting the mass of the black hole equal to one, $M = 1$, are used in order to obtain completely dimensionless formulae hereafter.

The locally non-rotating frames (LNRF) are given by the tetrad of 1-forms (Bardeen et al. 1972)

$$e^{(t)} = \left(\frac{\Sigma\Delta}{A}\right)^{1/2} dt, \quad e^{(\varphi)} = \left(\frac{A}{\Sigma}\right)^{1/2} \sin \theta (d\varphi - \omega dt), \quad (5)$$

$$e^{(r)} = \left(\frac{\Sigma}{\Delta}\right)^{1/2} dr, \quad e^{(\theta)} = \Sigma^{1/2} d\theta, \quad (6)$$

where

$$\omega = -\frac{g_{t\varphi}}{g_{\varphi\varphi}} = \frac{2ar}{A} \quad (7)$$

is the angular velocity of the LNRF relative to distant observers. For matter with a 4-velocity U^μ and angular velocity profile $\Omega(r, \theta)$ orbiting the Kerr black hole, the azimuthal component of its 3-velocity in the LNRF reads

$$\mathcal{V}^{(\varphi)} = \frac{U^\mu e_\mu^{(\varphi)}}{U^\nu e_\nu^{(t)}} = \frac{A \sin \theta}{\Sigma \sqrt{\Delta}} (\Omega - \omega). \quad (8)$$

2.1. Keplerian thin discs

In thin discs matter follows nearly circular equatorial geodetical orbits characterized by the Keplerian distributions of the angular velocity and the specific angular momentum (in the equatorial plane, $\theta = \pi/2$)

$$\Omega = \Omega_K(r; a) \equiv \frac{1}{(r^{3/2} + a)}, \quad (9)$$

$$\ell = \ell_K(r; a) \equiv \frac{r^2 - 2ar^{1/2} + a^2}{r^{3/2} - 2r^{1/2} + a}. \quad (10)$$

The azimuthal component of the Keplerian 3-velocity in the LNRF reads

$$\mathcal{V}_K^{(\varphi)}(r; a) = \frac{(r^2 + a^2)^2 - a^2\Delta - 2ar(r^{3/2} + a)}{r^2(r^{3/2} + a)\sqrt{\Delta}} \quad (11)$$

and formally diverges for $r \rightarrow r_+ = 1 + \sqrt{1 - a^2}$, where the black-hole event horizon is located. Its radial gradient is given by

$$\frac{\partial \mathcal{V}_K^{(\varphi)}}{\partial r} = -\frac{r^5 + a^4(3r + 2) - 2a^3 r^{1/2}(3r + 1)}{2\Delta^{3/2} \sqrt{r}(r^{3/2} + a)^2} - \frac{2a^2 r^2(2r - 5) - 2ar^{5/2}(5r - 9)}{2\Delta^{3/2} \sqrt{r}(r^{3/2} + a)^2}. \quad (12)$$

As shown by Aschenbach (2004, 2006), the velocity profile has two changes of the gradient sign (where $\partial \mathcal{V}_K^{(\varphi)} / \partial r = 0$) in the field of rapidly rotating Kerr black holes with $a > a_{c(K)} \doteq 0.9953$ (see Fig. 1).

2.2. Marginally stable tori

Perfect-fluid stationary and axisymmetric toroidal discs are characterized by the 4-velocity field $U^\mu = (U^t, 0, 0, U^\varphi)$ with $U^t = U^t(r, \theta)$, $U^\varphi = U^\varphi(r, \theta)$, and by distribution of the specific angular momentum $\ell = -U_\varphi / U_t$. The angular velocity of orbiting matter, $\Omega = U^\varphi / U^t$, is then related to ℓ by the formula

$$\Omega = -\frac{\ell g_{tt} + g_{t\varphi}}{\ell g_{t\varphi} + g_{\varphi\varphi}}. \quad (13)$$

The marginally stable tori are characterized by uniform distribution of the specific angular momentum

$$\ell = \ell(r, \theta) = \text{const.}, \quad (14)$$

and are fully determined by the spacetime structure through equipotential surfaces of the potential $W = W(r, \theta)$ defined by the relations (Abramowicz et al. 1978)

$$W - W_{\text{in}} = \ln \frac{U_t}{(U_t)_{\text{in}}}, \quad (U_t)^2 = \frac{g_{t\varphi}^2 - g_{tt}g_{\varphi\varphi}}{g_{tt}\ell^2 + 2g_{t\varphi}\ell + g_{\varphi\varphi}}; \quad (15)$$

the subscript “in” refers to the inner edge of the disc.

The LNRF orbital velocity of the torus is given by

$$\mathcal{V}_T^{(\varphi)} = \frac{A(\Delta - a^2 \sin^2 \theta) + 4a^2 r^2 \sin^2 \theta}{\Sigma \sqrt{\Delta}(A - 2a\ell r)} \ell. \quad (16)$$

For marginally stable tori it is enough to consider the motion in the equatorial plane, $\theta = \pi/2$. Formally, this velocity vanishes for $r \rightarrow \infty$ and $r \rightarrow r_+$, i.e., there must be a change of its radial gradient for any values of the parameters a and ℓ , contrary to

the case of Keplerian discs. The radial gradient of the equatorial LNRF velocity of $\ell = \text{const.}$ tori reads

$$\frac{\partial \mathcal{V}_T^{(\varphi)}}{\partial r} = \left\{ \frac{[\Delta + (r-1)r][r(r^2 + a^2) - 2a(\ell - a)]}{[r(r^2 + a^2) - 2a(\ell - a)]^2 \sqrt{\Delta}} - \frac{r(3r^2 + a^2)\Delta}{[r(r^2 + a^2) - 2a(\ell - a)]^2 \sqrt{\Delta}} \right\} \ell, \quad (17)$$

so it changes its orientation at radii determined for a given ℓ by the condition

$$\ell = \ell_{\text{ex}}(r; a) \equiv a + \frac{r^2[(r^2 + a^2)(r-1) - 2r\Delta]}{2a[\Delta + r(r-1)]}. \quad (18)$$

Of course, for both thick tori and Keplerian discs we must consider the limit on the disc extension given by the innermost stable orbit. For Keplerian discs this is the marginally stable geodesical orbit, $r_{\text{in}} \approx r_{\text{ms}}$, while for thick tori this is an unstable circular geodesic kept stable by pressure gradients and located between the marginally bound and the marginally stable geodesical orbits, $r_{\text{mb}} \lesssim r_{\text{in}} \lesssim r_{\text{ms}}$, with the radius being determined by the specific angular momentum $\ell = \text{const.} \in (l_{\text{ms}}, l_{\text{mb}})$ through the equation $\ell = \ell_{\text{K}}(r; a)$; ℓ_{ms} (ℓ_{mb}) denotes specific angular momentum of the circular marginally stable (marginally bound) geodesic.

Detailed discussion of Stuchlík et al. (2005) shows that two physically relevant changes of sign of $\partial \mathcal{V}_T^{(\varphi)}/\partial r$ in the tori occur for Kerr black holes with the rotational parameter $a > a_{\text{c(T)}} \doteq 0.99979$ (see Fig. 1). The interval of relevant values of the specific angular momentum $\ell \in (\ell_{\text{ms}}(a), \ell_{\text{ex(max)}}(a))$, where $\ell_{\text{ex(max)}}(a)$ corresponds to the local maximum of the function (18), grows with a growing up to the critical value of $a_{\text{c(mb)}} \doteq 0.99998$. For $a > a_{\text{c(mb)}}$, the interval of relevant values of $\ell \in (\ell_{\text{ms}}(a), \ell_{\text{mb}}(a))$ is narrowing with the rotational parameter growing up to $a = 1$, which corresponds to a singular case where $\ell_{\text{ms}}(a = 1) = \ell_{\text{mb}}(a = 1) = 2$. Notice that the situation becomes to be singular only in terms of the specific angular momentum; it is shown (see Bardeen et al. 1972) that for $a = 1$ both the total energy E and the axial angular momentum L differ at r_{ms} and r_{mb} , respectively, but their combination, $\ell \equiv L/E$, giving the specific angular momentum, coincides at these radii.

It should be stressed that in the Kerr spacetimes with $a > a_{\text{c(T)}}$, the ‘‘humpy’’ profile of $\mathcal{V}_T^{(\varphi)}(r; a)$ occurs closely above the center of relevant toroidal discs, at radii corresponding to stable circular geodesics of the spacetime, where the radial and vertical epicyclic frequencies are also well defined.

A physically reasonable way of defining a global quantity characterizing rotating fluid configurations in terms of the LNRF orbital velocity is to introduce, so-called, von Zeipel radius defined by the relation

$$\mathcal{R} \equiv \frac{\ell}{\mathcal{V}_{\text{LNRF}}^{(\varphi)}} = (1 - \omega\ell)\tilde{\varrho}, \quad (19)$$

which generalizes in another way as compared with (Abramowicz et al. 1995) the Schwarzschildian definition of the gyration radius $\tilde{\varrho}$ (Abramowicz et al. 1993). Note that, except for the Schwarzschild case $a = 0$, the von Zeipel surfaces, defined as the surfaces of $\mathcal{R}(r, \theta; a, \ell) = \text{const.}$, do not coincide with those introduced by Kozłowski et al. (1978) as the surfaces of constant ℓ/Ω .²

In the case of marginally stable tori the von Zeipel surfaces $\mathcal{R} = \text{const.}$ coincide with the equivelocity surfaces

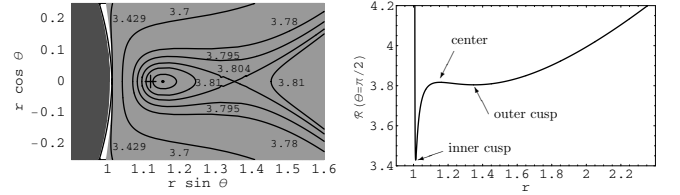
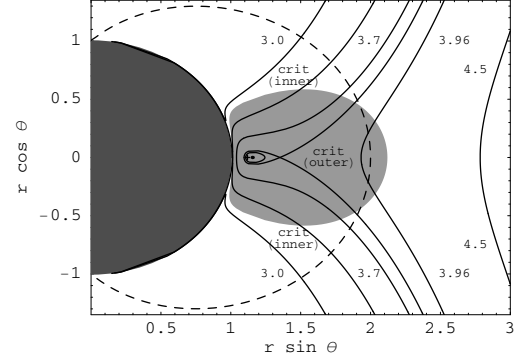


Fig. 2. Von Zeipel surfaces (meridional sections). For $a > a_{\text{c(T)}}$ and ℓ appropriately chosen, two surfaces with a cusp, or one surface with both the cusps, together with closed (toroidal) surfaces, exist, being located always inside the ergosphere (dashed surface) of a given spacetime. Both the outer cusp and the central ring of closed surfaces are located inside the toroidal equilibrium configurations corresponding to marginally stable thick discs (light-gray region; its shape is determined by the critical self-crossing equipotential surface of the potential $W(r, \theta)$). The cross (+) denotes the center of the torus. Dark region corresponds to the black hole. Figures illustrating all possible configurations of the von Zeipel surfaces are presented in Stuchlík et al. (2005). Here we present the figure plotted for the parameters $a = 0.99998$, $\ell = 2.0065$. Critical value of the von Zeipel radius corresponding to the inner and the outer self-crossing surface is $\mathcal{R}_{\text{c(in)}} \doteq 3.429$ and $\mathcal{R}_{\text{c(out)}} \doteq 3.804$, respectively, the central ring of toroidal surfaces corresponds to the value $\mathcal{R}_{\text{center}} \doteq 3.817$. Interesting region containing both the cusps and the toroidal surfaces is plotted in detail at the left lower figure. Right lower figure shows the behaviour of the von Zeipel radius in the equatorial plane.

$\mathcal{V}_T^{(\varphi)}(r, \theta; a, \ell) = \mathcal{V}_T^{(\varphi)} = \text{const.}$ Topology of the von Zeipel surfaces can be directly determined by the behaviour of the von Zeipel radius in the equatorial plane

$$\mathcal{R}(r, \theta = \pi/2; a, \ell) = \frac{r(r^2 + a^2) - 2a(\ell - a)}{r\sqrt{\Delta}}. \quad (20)$$

The local minima of the function (20) determine loci of the cusps of the von Zeipel surfaces, while its local maximum (if it exists) determines a circle around which closed toroidally shaped von Zeipel surfaces are concentrated (see Fig. 2). Notice that the minima (maximum) of $\mathcal{R}(r, \theta = \pi/2; a, \ell)$ correspond(s) to the maxima (minimum) of $\mathcal{V}_T^{(\varphi)}(r, \theta = \pi/2; a, \ell)$, therefore, the inner cusp is always physically irrelevant being located outside of the toroidal configuration of perfect fluid. Behaviour of the von Zeipel surfaces nearby the center and the inner edge of the thick discs orbiting Kerr black holes with $a > a_{\text{c(T)}} \doteq 0.99979$, i.e., the existence of the von Zeipel surface with an outer cusp or the surfaces with toroidal topology, suggests possible generation of instabilities in both the vertical and radial direction.

² For more details see Stuchlík et al. (2005).

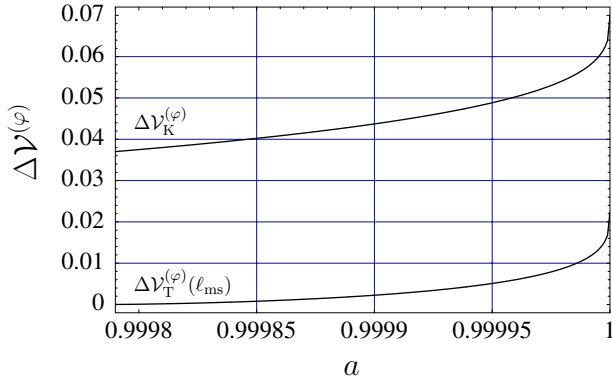


Fig. 3. Velocity difference $\Delta\mathcal{V}^{(\varphi)} = \mathcal{V}_{\max}^{(\varphi)} - \mathcal{V}_{\min}^{(\varphi)}$ as a function of the rotational parameter a of the black hole for both the thin (Keplerian) disc and the marginally stable (non-Keplerian) disc with $\ell = \ell_{\text{ms}}$.

2.3. Velocity profiles with a hump

Behavior of $\mathcal{V}_{\text{T}}^{(\varphi)}(r; a, \ell)$ and $\mathcal{V}_{\text{K}}^{(\varphi)}(r; a)$ is illustrated in Fig. 1. With a growing in the region of $a \in (a_{\text{c(T)}}, 1)$ ($a \in (a_{\text{c(K)}}, 1)$), the difference $\Delta\mathcal{V}_{\text{T}}^{(\varphi)} \equiv \mathcal{V}_{\text{T}(\max)}^{(\varphi)} - \mathcal{V}_{\text{T}(\min)}^{(\varphi)}$ ($\Delta\mathcal{V}_{\text{K}}^{(\varphi)} \equiv \mathcal{V}_{\text{K}(\max)}^{(\varphi)} - \mathcal{V}_{\text{K}(\min)}^{(\varphi)}$) grows (Fig. 3) as well as the difference of radii, $\Delta r_{\text{T}} \equiv r_{\text{T}(\max)} - r_{\text{T}(\min)}$ ($\Delta r_{\text{K}} \equiv r_{\text{K}(\max)} - r_{\text{K}(\min)}$), where the local extrema of $\mathcal{V}_{\text{T}}^{(\varphi)}$ ($\mathcal{V}_{\text{K}}^{(\varphi)}$) occur, see Fig. 4.

In terms of the redefined rotational parameter $(1 - a)$, the “humpy” profile of the LNRF orbital velocity of marginally stable thick discs occurs for discs orbiting Kerr black holes with $(1 - a) < 1 - a_{\text{c(T)}} \doteq 2.1 \times 10^{-4}$, which is more than one order lower than the value $1 - a_{\text{c(K)}} \doteq 4.7 \times 10^{-3}$ found by Aschenbach (2004) for the Keplerian thin discs. Moreover, in the thick discs, the velocity difference $\Delta\mathcal{V}_{\text{T}}^{(\varphi)}$ is smaller but comparable with those in the thin discs (see Fig. 3). In fact, we can see that for $a \rightarrow 1$, the velocity difference in the thick discs $\Delta\mathcal{V}_{\text{T}}^{(\varphi)} \approx 0.02$, while for the Keplerian discs it goes even up to $\Delta\mathcal{V}_{\text{K}}^{(\varphi)} \approx 0.07$.

3. Humpy frequency and its relation to epicyclic frequencies

In Kerr spacetimes, the frequencies of the radial and latitudinal (vertical) epicyclic oscillations related to an equatorial Keplerian circular orbit at a given r are determined by the formulae (e.g., Aliev & Galtsov 1981; Nowak & Lehr 1998)

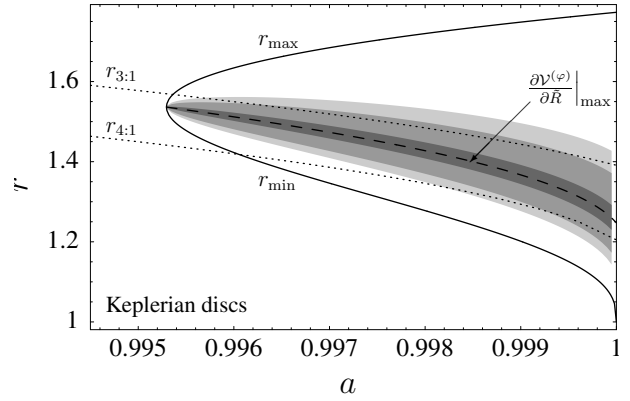
$$v_r^2 = v_{\text{K}}^2(1 - 6r^{-1} + 8ar^{-3/2} - 3a^2r^{-2}), \quad (21)$$

$$v_v^2 \equiv v_{\theta}^2 = v_{\text{K}}^2(1 - 4ar^{-3/2} + 3a^2r^{-2}), \quad (22)$$

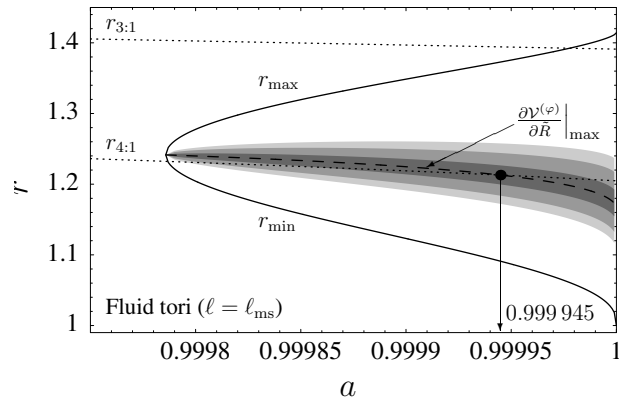
where $v_{\text{K}} = \Omega_{\text{K}}/2\pi$. A detailed analysis of properties of the epicyclic frequencies can be found in Török & Stuchlík (2005a,b). The epicyclic oscillations with the frequencies v_r, v_v can be related to both the thin Keplerian discs (Abramowicz & Kluźniak 2000; Kato 2005) and thick, toroidal discs (Rezzolla et al. 2003; Kluźniak et al. 2004b).

Aschenbach (2004, 2006) defined the characteristic (critical) frequency of any related mechanism possibly exciting the disc oscillations in the region of positive gradient of its LNRF-velocity $\mathcal{V}^{(\varphi)}$ by the maximum positive slope of $\mathcal{V}^{(\varphi)}$:

$$v_{\text{crit}}^A \equiv \left. \frac{\partial \mathcal{V}_{\text{K}}^{(\varphi)}}{\partial r} \right|_{\max}. \quad (23)$$



(a)



(b)

Fig. 4. Positions of local extrema of $\mathcal{V}^{(\varphi)}$ (in B-L coordinates) for Keplerian discs **a**) and marginally stable discs with $\ell = \ell_{\text{ms}}$ **b**) together with the locations of resonant orbits $r_{3:1}$ and $r_{4:1}$ (where the resonance between the vertical and radial epicyclic oscillations takes place) in dependence on the rotational parameter a of the black hole. Dashed curve corresponds to the maximum positive values of the LNRF orbital velocity gradient in terms of the proper radial distance where the critical frequency v_{crit}^A is defined, boundaries of shaded regions correspond to orbits where the velocity gradient giving the characteristic frequency, $\partial\mathcal{V}^{(\varphi)}/\partial\bar{R}$, reaches **a**) 99%, 90%, 80% and **b**) 99%, 95%, 90% of its maximum.

This frequency has to be determined numerically and we have done it for both the Keplerian discs and the marginally stable discs with $\ell = \ell_{\text{ms}} = \text{const.}$, see Fig. 5 and Table 1.

Although there is no detailed idea on the mechanism generating the “hump-induced” oscillations, it is clear that the Aschenbach proposal of defining the characteristic frequency deserves attention. It should be stressed, however, that a detailed analysis of the instability could reveal a difference between the characteristic frequency and the actual observable one, as the latter should be associated with the fastest growing unstable mode³. Moreover the frequency v_{crit}^A , defined by Eq. (23), represents an upper limit on the frequencies of the hump-induced oscillations, as it is given by maximum of the LNRF-velocity gradient in the humpy part of the velocity profile.

In the following we assume that the characteristic (critical) frequency is a typical frequency of oscillations induced by the conjectured “humpy instability”, and that the humpy oscillations could excite oscillations with the epicyclic frequencies or some combinational frequencies, if appropriate conditions for a forced

³ We thank to the referee for pointing out this possibility.

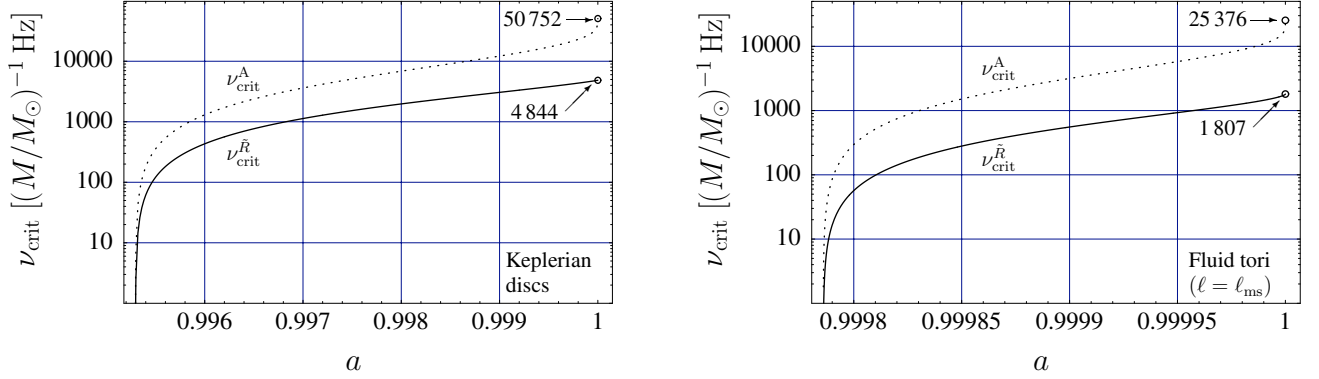


Fig. 5. Critical frequency ν_{crit}^A defined in terms of the B–L coordinate radius (Aschenbach 2004) and the physically correct (coordinate independent) critical frequency ν_{crit}^R defined in terms of the proper radial distance, as a function of the rotational parameter a of the black hole.

Table 1. Characteristic frequencies in units of $(M/M_\odot)^{-1}$ Hz (M/M_\odot is the mass of the Kerr black hole in units of mass of the Sun), corresponding to critical frequencies ν_{crit}^A , ν_∞^A , ν_{crit}^R , ν_∞^R defined in the text, are given for appropriate values of the black-hole spin. Maximal values of the frequencies related to the stationary observer at infinity are bold-faced. Note that only the frequencies ν_∞^R have physical meaning for direct comparison with the frequencies of orbital oscillations ν_{orb} , ν_r , ν_v related to the observers at infinity.

| $1 - a$ | Keplerian discs | | | | Fluid tori | | | |
|----------------------|-----------------------|----------------|-----------------------|----------------|-----------------------|----------------|-----------------------|----------------|
| | ν_{crit}^A | ν_∞^A | ν_{crit}^R | ν_∞^R | ν_{crit}^A | ν_∞^A | ν_{crit}^R | ν_∞^R |
| 4.5×10^{-3} | 356 | 86 | 121 | 29 | | | | |
| 4×10^{-3} | 1303 | 303 | 432 | 102 | | | | |
| 3×10^{-3} | 3617 | 767 | 1130 | 248 | | | | |
| 1×10^{-3} | 12 179 | 1849 | 3061 | 536 | | | | |
| 5×10^{-4} | 17 132 | 2126 | 3789 | 592 | | | | |
| 2×10^{-4} | 22 982 | 2203 | 4352 | 607 | 296 | 34 | 57 | 7 |
| 1×10^{-4} | 26 857 | 2126 | 4579 | 603 | 3160 | 315 | 555 | 61 |
| 1×10^{-5} | 36 593 | 1565 | 4816 | 590 | 10 940 | 657 | 1447 | 135 |
| 1×10^{-6} | 42 556 | 1001 | 4841 | 588 | 16 271 | 589 | 1718 | 147 |
| 1×10^{-9} | 49 250 | 201 | 4844 | 588 | 23 277 | 185 | 1807 | 150 |

resonance are satisfied in vicinity of the radius where the humpy oscillations occur.

In situations where the general relativity is crucial, it is necessary to consider $\partial\mathcal{V}^{(\varphi)}/\partial\tilde{R}$, where \tilde{R} is the physically relevant (coordinate-independent) proper radial distance, as this is an appropriate way for estimating the characteristic frequencies related to local physics in the disc. Then correct general relativistic definition of the critical frequency for possible excitation of oscillations in the disc is given by the relations

$$\nu_{\text{crit}}^{\tilde{R}} = \left. \frac{\partial\mathcal{V}^{(\varphi)}}{\partial\tilde{R}} \right|_{\text{max}}, \quad d\tilde{R} = \sqrt{g_{rr}} dr = \sqrt{\frac{\Sigma}{\Delta}} dr, \quad (24)$$

where $\mathcal{V}^{(\varphi)} = \mathcal{V}_K^{(\varphi)}(r; a)$ in thin Keplerian discs, and $\mathcal{V}^{(\varphi)} = \mathcal{V}_T^{(\varphi)}(r; l, a)$ in marginally stable thick discs. Of course, such a locally defined frequency, confined naturally to the observers orbiting the black hole with the LNRF, should be further related to distant stationary observers by the formula (taken at the B–L coordinate r corresponding to $(\partial\mathcal{V}^{(\varphi)}/\partial\tilde{R})_{\text{max}}$)

$$\nu_h = \nu_\infty^{\tilde{R}} = \sqrt{-(g_{tt} + 2\omega g_{t\varphi} + \omega^2 g_{\varphi\varphi})} \nu_{\text{crit}}^{\tilde{R}}. \quad (25)$$

We suggest to call such a coordinate-independent and, in principle, observable frequency the ‘‘humpy frequency’’, as it is related to the humpy profile of $\mathcal{V}^{(\varphi)}$, and denote it ν_h . Again, the physically relevant humpy frequency $\nu_h = \nu_\infty^{\tilde{R}}$, connected to observations by distant observers and exactly defined by Eqs. (24) and (25), represents an upper limit on characteristic frequencies

of oscillations induced by the hump of the LNRF-velocity profile, and the realistic humpy frequencies, as observed by distant observers, can be expected close to but smaller than $\nu_\infty^{\tilde{R}}$. Further, we denote r_h the B–L radius of definition of the humpy oscillations frequency, where $\partial\mathcal{V}^{(\varphi)}/\partial\tilde{R} = (\partial\mathcal{V}^{(\varphi)}/\partial\tilde{R})_{\text{max}}$. Of course, in realistic situations the hump-induced oscillation mechanism could work at the vicinity of r_h , with slightly different frequencies; we should take into account that the shift of the radius, where the mechanism works, shifts both the locally measured (LNRF) frequency (Eq. (24)) and the frequency related to distant observers (Eq. (25)). The zones of radii, where the critical frequency $\nu_{\text{crit}}^{\tilde{R}}$ differs up to 1%, 10% and 20% of its maximal value (given by $(\partial\mathcal{V}^{(\varphi)}/\partial\tilde{R})_{\text{max}}$) for thin (Keplerian) discs or 1%, 5% and 10% of its maximum for marginally stable discs with $\ell = \ell_{\text{ms}}$, are given in Fig. 4.

An analogical relation to Eq. (25) can be written also for the Aschenbach critical frequency ν_{crit}^A , giving the Aschenbach frequency related to distant observers ν_∞^A . Because the velocity gradient related to the proper distance \tilde{R} is suppressed in comparison with that related to the Boyer-Lindquist coordinate distance r , there is $\nu_{\text{crit}}^{\tilde{R}} < \nu_{\text{crit}}^A$. The situation is illustrated in Fig. 5. Moreover, Fig. 6 shows mutual behaviour of the ‘‘coordinate’’ and ‘‘proper’’ radial gradient $\partial\mathcal{V}^{(\varphi)}/\partial r$ and $\partial\mathcal{V}^{(\varphi)}/\partial\tilde{R}$ in the region between the local minimum and the outer local maximum of the orbital velocity $\mathcal{V}^{(\varphi)}$ of $\ell = \ell_{\text{ms}} = \text{const.}$ discs for an appropriately chosen value of the rotational parameter a . It is interesting to compare the Aschenbach frequencies (defined in terms

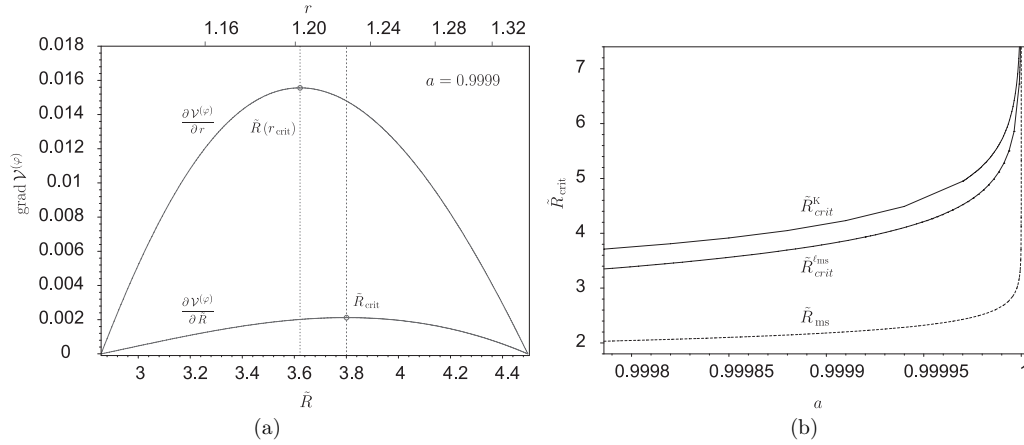


Fig. 6. Determination of the critical “humpy” frequency. **a)** Positive parts of the “coordinate” and “proper” radial gradient $\partial\mathcal{V}^{(\varphi)}/\partial r$ and $\partial\mathcal{V}^{(\varphi)}/\partial\tilde{R}$ for a given value of the rotational parameter a in the Keplerian disc. **b)** Proper radial distance of the loci of $(\partial\mathcal{V}^{(\varphi)}/\partial\tilde{R})_{\max}$ measured from the marginally bound orbit for both the Keplerian discs ($\tilde{R}_{\text{crit}}^{\text{K}}$) and $\ell = \ell_{\text{ms}}$ perfect-fluid tori ($\tilde{R}_{\text{crit}}^{\text{ms}}$). Proper radial distance to the marginally stable orbit (\tilde{R}_{ms}) is also shown.

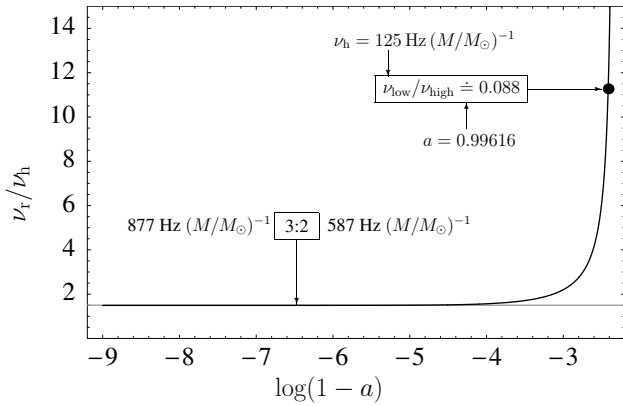


Fig. 7. Spin dependence of the ratio of the radial epicyclic frequency and the “humpy frequency” related to distant observers. The ratio is given in the radius of definition of the humpy frequency r_h . In the interval of $1 - a \in (1.7 \times 10^{-3}, 10^{-4})$, the ratio rapidly falls down, to the asymptotic value of 3:2 starting at $a \sim 10^{-4}$. Then an exact $1/M$ scaling holds with frequencies depicted in the figure. Notice that at the Aschenbach’s value of $a \approx 0.99616$, for which the resonant orbit with $\nu_v:\nu_r \sim 3:1$ is close to r_h , there is $\nu_r/\nu_h \sim 12$, analogous to the ratio of high and low frequency QPOs.

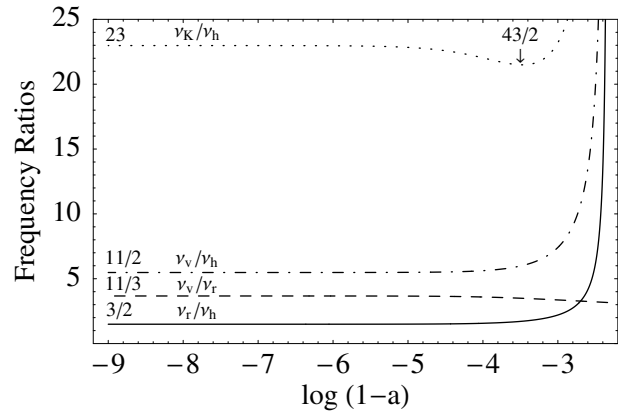


Fig. 8. Spin dependence of the ratios of the radial (ν_r) and vertical (ν_v) epicyclic frequencies, and the Keplerian frequency (ν_K) to the thin-disc humpy frequency related to distant observers (ν_h). Further the ratio of the epicyclic frequencies is given at the radius of definition of the humpy frequency. All the frequency ratios are asymptotically (for $1 - a < 10^{-4}$) constant. There is $\nu_K:\nu_v:\nu_r:\nu_h \sim 46:11:3:2$. Therefore, we can expect some resonant phenomena on the ratio of $\nu_r:\nu_h \sim 3:2$, and $\nu_K:\nu_v \sim 4$ that could be both correlated.

of the B-L coordinate r) with the critical frequencies defined in terms of the proper radial distance \tilde{R} . Characteristic frequencies $\nu_{\text{crit}}^{\text{A}}$, ν_{∞}^{A} , $\nu_{\text{crit}}^{\text{R}}$, ν_{∞}^{R} are given in Table 1 for some typical values of the rotational parameter a for both Keplerian discs and limiting $\ell = \text{const.}$ tori with $\ell = \ell_{\text{ms}}$.

The physically and observationally relevant frequency connected to the LNRF-velocity gradient sign change is given by the frequency $\nu_h = \nu_{\infty}^{\text{R}}$ corresponding to the locally “hump-induced” oscillations taken from the point of view of distant stationary observers. In order to obtain an intuitive insight into a possible observational relevance of ν_h , it is useful to compare it with the frequencies of the radial and vertical epicyclic oscillations, ν_r and ν_v , and the orbital frequency of the disc, $\nu_{\text{orb}} = \Omega/2\pi$, where Ω is given for both thin and thick discs by Eq. (13) and the appropriate distribution of the specific angular momentum ℓ . The most interesting and crucial phenomenon is the spin independence of the frequency ratios for extremely rapid Kerr black holes. The results are given in Figs. 7–10. Further we can see

(Figs. 4) that the resonant epicyclic frequencies radii $r_{3:1}$ and $r_{4:1}$ are located within the zone of the hump-induced oscillation mechanism in both thin discs and marginally stable tori.

We would like to call attention to the fact that in Keplerian discs the sign changes of the radial gradient of the orbital velocity in LNRF occur nearby the $r = r_{3:1}$ orbit (with $\nu_v:\nu_r = 3:1$), while in the vicinity of the $r = r_{3:2}$ orbit (with $\nu_v:\nu_r = 3:2$), $\partial\mathcal{V}^{(\varphi)}/\partial r < 0$ for all values of a for both Keplerian discs and marginally stable tori with all allowed values of ℓ . The parametric resonance, which is the strongest one for the ratio of the epicyclic frequencies $\nu_v:\nu_r = 3:2$, can occur at the $r = r_{3:2}$ orbit, while its effect is much smaller at the radius $r = r_{3:1}$, as noticed by Abramowicz et al. (2003). Nevertheless, the forced resonance may take place at the $r_{3:1}$ orbit. Notice that the forced resonance at $r = r_{3:1}$ can generally result in observed QPOs frequencies with 3:2 ratio due to the beat frequencies allowed for the forced resonance as shown in Abramowicz et al. (2004). But the forced resonance at $r_{3:1}$ between the epicyclic frequencies, induced by the humpy profile of $\mathcal{V}^{(\varphi)}$, seems to be irrelevant

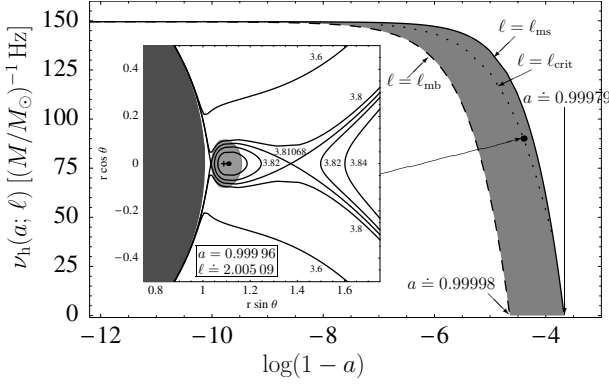


Fig. 9. Interval of humpy frequencies for the marginally stable thick discs with $\ell \in (\ell_{ms}, \ell_{mb})$ as a function of the black-hole spin a . For $a \rightarrow 1$, the interval is narrowing and asymptotically reaching the value of $150 \text{ Hz } (M/M_\odot)^{-1}$. Dotted curve corresponds to the humpy frequencies of marginally stable slender tori with $\ell = \ell_{crit}$, for which the critical von Zeipel surface contains two cusps (as it is demonstrated for one special case in the left panel of the figure; the thick part of the torus is given by the light-gray region).

in the case of microquasars, since all observed frequencies lead to the values of the rotational parameter $a < a_{c(K)}$, as shown by Török et al. (2005). On the other hand, the LNRF-velocity hump could induce the forced resonance between another (non-epicyclic) frequencies as well, and thus being relevant also for microquasars like the nearly extreme Kerr black hole candidate GRS 1915+105 (McClintock et al. 2006).

The marginally stable tori have a structure that depends on the value of the specific angular momentum $\ell \in (\ell_{ms}, \ell_{mb})$. The oscillations of slender tori ($\ell \approx \ell_{ms}$) have frequencies equal to the epicyclic frequencies relevant for test particle motion, but the frequencies of non-slender tori are different, as shown for pseudo-Newtonian tori (Šrámková 2005; Blaes et al. 2006) and expected for tori in the strong gravitational field of Kerr black holes. Therefore, comparison of the humpy frequencies and the epicyclic frequencies is relevant for the slender tori only.

The humpy frequency is defined for all $a > 0.99979$ and all $\ell \in (\ell_{ms}, \ell_{mb})$, see Fig. 9. It is important that in the field of Kerr black holes with $1 - a < 10^{-8}$, there is $\nu_h(a, \ell) \approx 150 \text{ Hz } (M/M_\odot)^{-1}$ independently of a and ℓ . Further, it is shown that physically important case of tori admitting evolution of toroidal von Zeipel surfaces with the critical surface self-crossing in both the inner and the outer cusps is allowed at $\ell = \ell_{crit}$, where $\ell_{crit} \gtrsim \ell_{ms}$ only slightly differs from ℓ_{ms} , i.e., such tori can be slender, see Fig. 9. The ratios of ν_r/ν_h , ν_v/ν_h and ν_o/ν_h are given for the tori with $\ell \approx \ell_{ms}$ in Fig. 10. Their asymptotical values, valid for $1 - a < 10^{-6}$, are independent of both a and ℓ .

4. Concluding remarks

The equality of ν_{crit}^A and ν_r for the Kerr black holes with $a \approx 0.99616$, indicating direct relation of the Aschenbach characteristic frequency and the radial epicyclic frequency (Aschenbach 2004, 2006), is rather only an accidental coincidence, because ν_{crit}^A is defined in a coordinate-dependent way. The physically relevant frequency $\nu_h = \nu_\infty^R$ cannot be directly related to the radial epicyclic frequency in Keplerian discs, as $\nu_\infty^R < \nu_r$ for all relevant values of $a \in (a_{c(K)}, 1)$. Nevertheless, the behaviour

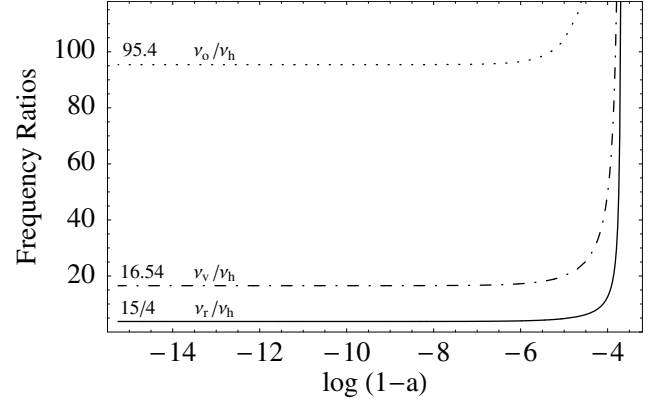


Fig. 10. Spin dependence of the ratios of the radial (ν_r) and vertical (ν_v) epicyclic frequencies, and the orbital frequency (ν_o) of the marginally stable $\ell = \ell_{ms}$ disc to the thick-disc humpy frequency related to distant observers (ν_h). All the frequency ratios are asymptotically (for $1 - a < 10^{-6}$) almost constant.

of the ratio ν_r/ν_∞^R indicates some interesting consequences (see Fig. 7).

First, for thin (Keplerian) discs around the Kerr black holes with $a \approx 0.99616$, when the ratio of epicyclic frequencies $\nu_v:\nu_r \sim 3:1$ at the radius of definition of ν_∞^R , we find $\nu_r:\nu_\infty^R \sim (11-13):1$, i.e., in such a situation the frequency induced by the positive gradient of the LNRF-velocity profile could be related to the low-frequency oscillations. However, such explanation is restricted to extremely rapidly rotating black holes and, contrary to the idea of the 13th wave (Abramowicz et al. 2004), cannot be extended to other black-hole, neutron-star, and white-dwarf systems. Therefore, this has to be taken as a kind of curiosity working for a very special class of black-hole systems only.

Second, for thin (Keplerian) discs around the Kerr black holes with $a > 0.9999$, there is the ratio of $\nu_r:\nu_\infty^R \sim 3:2$, and $\nu_v:\nu_\infty^R \sim 11:2$, independently of a . Assuming that the oscillations at the humpy frequency $\nu_h = \nu_\infty^R$ could be really directly detected by distant observers, for such black holes with $1 - a < 10^{-4}$ the high-frequency twin peak QPOs with 3:2 ratio could be explained independently of the standard resonant phenomena, if we focus on the asymptotic behaviour of $\nu_r:\nu_\infty^R \sim 3:2$. Moreover, for such extremely rapid Kerr black holes with $1 - a < 10^{-4}$, we could consider triples of frequencies taken in rational ratios $\nu_v:\nu_r:\nu_\infty^R \sim 11:3:2$, if the epicyclic oscillations are excited by the LNRF-velocity hump. Such frequency ratios could be observed mainly in disc systems around supermassive black holes in galactic nuclei that are expected to be extremely fast rotating; especially Sgr A* should be tested very carefully for this possibility. For Kerr black holes with the spin parameter $1 - a > 10^{-4}$, the frequency ratio is different and depends strongly on the spin a (see Figs. 7 and 8).

Considering also the Keplerian frequency we find the ratio of $\nu_K:\nu_\infty^R$ having a local minimum for $a \approx 0.99965$ and a nearly constant value for $1 - a < 10^{-5}$, where $\nu_K:\nu_\infty^R \sim 23$. In the field of Kerr black holes with $1 - a < 10^{-5}$, the frequency ratios $\nu_K:\nu_v:\nu_r:\nu_\infty^R \sim 46:11:3:2$ are almost independent of a . Thus for the extremely rapid Kerr black holes the $1/M$ scaling of considered frequencies is quite exact. Note that in such a case there is $\nu_r:\nu_h \sim 3:2$ and the ratio $\nu_K:\nu_v$ is close to the ratio 4:1 at the radius of definition of the humpy frequency. This indicates a possibility of “doubled” resonant phenomena with the special

frequency ratios in Keplerian discs orbiting extremely rapid Kerr black holes ($1 - a < 10^{-5}$).

Third, the hump-induced oscillations with frequencies $\nu_h \leq \nu_\infty^{\tilde{R}}$ could be generated in a zone around r_h ($\nu_h = \nu_\infty^{\tilde{R}}$ at r_h), where the resonant phenomena between the radial and vertical epicyclic oscillations could enter the game, namely at the ratios of $\nu_v:\nu_r = 3:1$ and $4:1$. Interesting resonant phenomena could be then expected when the $\nu_r:\nu_h$ corresponds to the ratio of small integer numbers. Especially the case of $\nu_r:\nu_h \sim 3:2$ in spacetimes with $1 - a < 10^{-4}$ is worth of attention. In general, observationally relevant should be the resonances represented by frequency ratios in small integer numbers $p:q$. As shown in Landau & Lifshitz (1973), the relevance of resonant phenomena depends on the order of resonance $n = \max(p, q)$, and falls steeply (in powers) with increasing value of n ; in fact they argue that relevant resonant phenomena could be expected for $n \leq 4$. Therefore, the frequency ratios such as $23:1$, $11:2$, $11:3$ appear to be quite irrelevant in realistic resonance models.

Recall that there is a well known Thorne limit giving the maximum spin of the Kerr black hole in systems with thin accretion discs, $a_{\max} \approx 0.998$, determined by the back-reaction of photons radiated from the disc and captured by the black hole (Page & Thorne 1974; Thorne 1974). If the hump-induced oscillations and related epicyclic frequencies will be observed in ratios corresponding to the asymptotic region of $a > 0.9999$ for Keplerian discs, the Thorne model should be corrected, e.g., by effect of an occultation of the disc. In the case for which the Thorne limit turns out to be realistic, the hump-induced oscillations have to be restricted on the spin interval $a \in (0.9953, 0.998)$. We expect the Thorne limit being relevant for smooth thin discs, while the overcoming of a_{\max} could be expected in highly turbulent discs with toroidal internal parts.

For thick discs the situation is much more complex, being dependent on both the rotational parameter (spin) a and the specific angular momentum ℓ . The range of maximal humpy frequencies for a given spin a is plotted in Fig. 9 and is determined by their evaluation in limiting values of the specific angular momentum ℓ relevant for the “humpy” effect in marginally stable thick accretion discs (see the discussion in Sect. 2.2). The minimal value corresponds to $\ell_{\text{ms}}(a)$ while the maximal value, in dependence of a , corresponds to $\ell_{\text{ex(max)}}(a)$ (for $0.99979 \leq a \leq 0.99998$) or $\ell_{\text{mb}}(a)$ (for $0.99998 \leq a \leq 1$). Notice that asymptotically (for $1 - a < 10^{-8}$) both $\nu_{\text{h(ms)}}$ and $\nu_{\text{h(mb)}}$ coincide on the line of $150 \text{ Hz } (M/M_\odot)^{-1}$. Clearly, the same is true for the humpy frequencies related to discs with any relevant $\ell \in (\ell_{\text{ms}}, \ell_{\text{mb}})$. The spin-dependence of the ratio of the humpy frequency and the epicyclic and orbital frequencies (taken at the radius of definition of the humpy frequency) for the case of limiting $\ell = \ell_{\text{ms}}$ discs is given in Fig. 10. Again we obtain asymptotically constant (spin-independent) ratios for black holes with $1 - a < 10^{-6}$, where $\nu_r:\nu_{\text{h(ms)}} \sim 15:4$, $\nu_v:\nu_r \doteq 4.39$, $\nu_v:\nu_{\text{h(ms)}} \doteq 16.54$, $\nu_{\text{orb}}:\nu_r \doteq 25.4$, and $\nu_{\text{orb}}:\nu_h \doteq 95.4$. It should be stressed that for the holes with $1 - a < 10^{-6}$ the same ratios with the humpy frequencies are obtained for the discs with any $\ell \in (\ell_{\text{ms}}, \ell_{\text{mb}})$, as $\ell_{\text{mb}} \rightarrow \ell_{\text{ms}} \rightarrow 2$ for $a \rightarrow 1$. The asymptotically constant values of the frequency ratios correspond to the rational value only in the case of $\nu_r:\nu_h \sim 15:4$. Of course, we could find some rational ratios for any ones, if $1 - a > 10^{-6}$. On the other hand, we directly see (Fig. 4b) that for the very slender marginally stable tori ($\ell \approx \ell_{\text{ms}}$) the resonant phenomena on epicyclic frequencies with $\nu_v:\nu_r = 4:1$ ratio appear in very close vicinity of the humpy radius r_h , making thus a very special prediction on the QPOs frequencies observed in such hypothetical systems with Kerr black

holes having $1 - a < 2 \times 10^{-4}$. In the marginally stable slender tori the resonant phenomena between the radial epicyclic and humpy oscillations, taking place at the humpy radius r_h , and between the vertical and radial epicyclic oscillations near the humpy radius, both with the ratio $\sim 4:1$, could be observationally relevant only, but their relevance is expected to be lower than that of the frequency ratios $3:2$ and $3:1$ in Keplerian discs.

Finally, it should be stressed that at present no direct mechanism triggering the LNRF velocity hump excited oscillations is known, being a challenge for investigation, since the existence of the toroidal von Zeipel surfaces (see Figs. 2, 9) brings some indication of possible triggering of instabilities in both radial and vertical directions leading to oscillations in accretion discs. The predictions for the ratio of the humpy and epicyclic or Keplerian (orbital) frequencies presented here for both thin discs and slender tori have to be compared with observations made in nearly extreme Kerr black hole systems. In the case of the humpy oscillations excited systems we could observe more than two QPOs with frequencies in rational ratio. It seems that in the X-ray variable binary system (microquasar) with the nearly extreme Kerr black hole candidate GRS 1915+105 four oscillations with related frequencies have been observed, what brings a large field for testing the predictions of the “LNRF-velocity hump excited oscillations” model. The tests have to be done in a close connection to both the related resonance model and the results of the spectral analysis of the X-ray continuum, as observed in GRS 1915+105 (Remillard 2005; McClintock et al. 2006)⁴. We believe that a synergy effect of such studies could lead to deeper understanding of X-ray binary systems, namely microquasars.

Acknowledgements. This work was supported by the Czech grant MSM 4781305903.

References

- Abramowicz, M. A., & Kluźniak, W. 2000, *ApJ*, 374, L19
 Abramowicz, M. A., Jaroszyński, M., & Sikora, M. 1978, *A&A*, 63, 221
 Abramowicz, M. A., Miller, J. C., & Stuchlík, Z. 1993, *Phys. Rev. D*, 47, 1440
 Abramowicz, M. A., Nurowski, P., & Wex, N. 1995, *Classical Quantum Gravity*, 12, 1467
 Abramowicz, M. A., Karas, V., Kluźniak, W., Lee, W., & Rebusco, P. 2003, *PASJ*, 55, 467
 Abramowicz, M. A., Kluźniak, W., Stuchlík, Z., & Török, G. 2004, in *Proceedings of RAGtime 4/5: Workshops on black holes and neutron stars*, Opava, 14–16/13–15 Oct. 2002/03, ed. S. Hledík & Z. Stuchlík (Opava: Silesian University in Opava)
 Aliev, A. N., & Galtsov, D. V. 1981, *Gen. Relativity Gravitation*, 13, 899
 Aschenbach, B. 2004, *A&A*, 425, 1075
 Aschenbach, B. 2006 [arXiv:astro-ph/0603193]
 Aschenbach, B., Grosso, N., Porquet, D., & Predehl, P. 2004, *A&A*, 417, 71
 Bardeen, J. M., Press, W. H., & Teukolsky, S. A. 1972, *ApJ*, 178, 347
 Benjamin, T. B., & Feir, J. E. 1967, *J. Fluid Mechanics*, 27, 417
 Blaes, O., Šrámková, E., Abramowicz, M. A., Kluźniak, W., & Torkelson, U. 2006, *ApJ*, submitted
 Genzel, R., Schoedel, R., Ott, T., et al. 2003, *Nature*, 425, 934
 Ghez, A. M. 2004, in *Coevolution of Black Holes and Galaxies* (Carnegie Observatories Astrophysics Series), ed. L. C. Ho (Cambridge University Press), 53
 Kato, S. 2001, *PASJ*, 53, L37
 Kato, S. 2005, *PASJ*, 56, L25
 Kluźniak, W., & Abramowicz, M. A. 2001, *Acta Phys. Polonia B*, 32, 3605
 Kluźniak, W., Abramowicz, M. A., Kato, S., Lee, W. H., & Stergioulas, N. 2004a, *ApJ*, 603, L89

⁴ If the results of Aschenbach et al. (2004) will be confirmed by more precise observations, the Galactic Center black hole system Sgr A* could serve as another example of the nearly extreme Kerr black hole system with more than two QPO oscillations observed that could test the “humpy” model.

- Kluźniak, W., Abramowicz, M. A., & Lee, W. H. 2004b, in *X-Ray Timing 2003: Rossi and Beyond*, ed. P. Kaaret, F. K. Lamb, & J. H. Swank (Melville, NY: AIP) [arXiv:astro-ph/0402013]
- Kozłowski, M., Jaroszynski, M., & Abramowicz, M. A. 1978, *A&A*, 63, 209
- Landau, L. D., & Lifshitz, J. M. 1973, *Teoretičeskaja fizika*, Vol. I, *Mechanika*, 3rd Ed. (Moskva: Nauka)
- Mauche, C. W. 2002, *ApJ*, 580, 423
- McClintock, J. E., & Remillard, R. A. 2004, in *Compact Stellar X-Ray Sources*, ed. W. H. G. Lewin, & M. van der Klis (Cambridge: Cambridge University Press)
- McClintock, J. E., Shafee, R., Narayan, R., et al. 2006, *ApJ*, submitted [arXiv:astro-ph/0606076]
- Nowak, M. A., & Lehr, D. E. 1998, in *Theory of Black Hole Accretion Disks*, ed. M. A. Abramowicz, G. Björnsson, & J. E. Pringle (Cambridge: Cambridge University Press), 233
- Page, D. N., & Thorne, K. S. 1974, *ApJ*, 191, 499
- Psaltis, D., Belloni, T., & van der Klis, M. 1999, *ApJ*, 520, 262
- Remillard, R. A. 2005, *Astron. Nachr.*, 326, 804
- Rezzolla, L., Yoshida, S., Maccarone, T. J., & Zanotti, O. 2003, *MNRAS*, 344, L37
- Stuchlík, Z., Slaný, P., & Török, G. 2004, in *Proc. of RAGtime 4/5: Workshops on black holes and neutron stars*, Opava, 14–16/13–15 Oct. 2002/03, ed. S. Hledík, & Z. Stuchlík (Opava: Silesian University in Opava), 239, in press
- Stuchlík, Z., Slaný, P., Török, G., & Abramowicz, M. A. 2005, *Phys. Rev. D*, 71, 024037
- Šrámková, E. 2005, *Astron. Nachr.*, 326, 835
- Thorne, K. S. 1974, *ApJ*, 191, 507
- Török, G. 2005, *Astron. Nachr.*, 326, 856
- Török, G., & Stuchlík, Z. 2005a, in *Proceedings of RAGtime 6/7: Workshop on black holes and neutron stars*, Opava, September 2004/2005, ed. S. Hledík, & Z. Stuchlík
- Török, G., & Stuchlík, Z. 2005b, *A&A*, 437, 775
- Török, G., Abramowicz, M. A., Kluźniak, W., & Stuchlík, Z. 2005, *A&A*, 436, 1
- Török, G., Abramowicz, M., Kluźniak, W., & Stuchlík, Z. 2006, in *Proceedings of the Albert Einstein Century International*, American Institut of Physics (American Institut of Physics), in print
- van der Klis, M. 2000, *ARA&A*, 38, 717
- Warner, B., Woudt, P. A., & Pretorius, M. L. 2003, *MNRAS*, 344, 1193